SCIENTIFIC REPORTS

OPEN

SUBJECT AREAS:
SPINTRONICS
ELECTRONIC PROPERTIES AND DEVICES

Received
10 April 2014

Accepted
20 August 2014

Published
10 September 2014

Correspondence and requests for materials should be addressed to W.X.Z. (zhangwenxing@tyut.edu.cn)

Voltage-driven spintronic logic gates in graphene nanoribbons

WenXing Zhang

Key Lab of Advanced Transducers and Intelligent Control System of Ministry of Education, TaiYuan University of Technology, TaiYuan, ShanXi 030024, China.

Electronic devices lose efficacy due to quantum effect when the line-width of gate decreases to sub-10 nm. Spintronics overcome this bottleneck and logic gates are building blocks of integrated circuits. Thus, it is essential to control electronic transport of opposite spins for designing a spintronic logic gate, and spin-selective semiconductors are natural candidates such as zigzag graphene nanoribbons (ZGNR) whose edges are ferromagnetically ordered and antiferromagnetically coupled with each other. Moreover, it is necessary to sandwich ZGNR between two ferromagnetic electrodes for making a spintronic logic gate and also necessary to apply magnetic field to change the spin orientation for modulating the spin transport. By first principle calculations, we propose a method to manipulate the spin transport in graphene nanoribbons with electric field only, instead of magnetic field. We find that metal gates with specific bias nearby edges of ZGNR build up an in-plane inhomogeneous electric field which modulates the spin transport by localizing the spin density in device. The specific manipulation of spin transport we have proposed doesn't need spin-charge conversion for output and suggests a possible base for designing spintronic integrated circuit in atomic scale.

More than thirty years ago, it has been proposed that quantum effect can be used for calculations[1] and lots of experimental and theoretical studies on spintronics emerged[2]. For spintronic logic gates, ZGNR can be used as both devices and leads due to its spin-selectivity[3–5] and tunability by electric field[6–8]. However, it limits the feasibility that ferromagnetic electrodes and magnetic field are used in spintronic logic gates to manipulate the spin transport[9–11]. Thus, it remains unknown to manipulate the spin transport for logic operations ('AND', 'OR', 'NOT') with applied electric field directly. Here we show a method of utilizing only electric field to tune spin transport in ZGNR, and design a prototype of spintronic logic gate by first-principle calculations.

In experiments, graphene nanoflakes (GNF) have been fabricated and observed[12–15]. For GNF samples, zigzag-shaped edges are more favorable than armchair-shaped edges in energy due to less dangling bonds. Selected graphene flakes are further processed into multi-terminal devices[16–18]. An ideal zigzag-shaped edge of ribbon-like GNF is ferromagnetically ordered[19]. In real GNF, unordered defects at edges localize the magnetism of edge states, although there are lots of Dirac fermions in bulk[20–22]. Both good quality with less defects and accurate measurements are needed to seek the ferromagnetism at edges in GNF. It is reported recently that spin-polarized transport at edges in ribbon-like GNF have been observed[23]. The experiment (Ref. 23) has shown a new kind of one-dimensional electronic system with a tunable band gap and a spatially separated spin texture due to breaking the symmetry of planar spin-rotations under a very large magnetic field angled with respect to the graphene plane. In principle, the spin texture of ZGNR can be modulated not only by the symmetry breaking in magnetic field but also by a lot of other factors such as external electric field[4–6], magnetic impurities[24,25], substrate adsorption[26], and other structure defects[27,28]. Here we propose a prototype of quantum logic gates based on the following mechanism: Spin polarized states in the vicinity of Fermi level (E_F) are localized at edges of GNF, so an external electric field localized nearby the edge can be used to tune the distribution of spin density and tune the spin transport correspondingly.

A graphene nanoribbon with four zigzag chains (4ZGNR) is used to construct the logic gate whose size is much smaller than the gate line-width of current CPUs. At each edge of 4ZGNR, two metal gates are established and a dielectric region is inserted to divide the external potential at the edge into three parts (Fig. 1a). For our model, the dielectric constant of dielectric region is set to $4.5\varepsilon_0$ similar to silicon. Our study of the spin-resolved electronic structure of 4ZGNR in electric field is based on ab initio local spin density approximation[29] (ab initio LSDA) and norm-conserving pseudo-potentials. Transport properties of the logic gate are studied with non-equilibrium green's function (NEGF) technique using Double Zeta Polarized (DZP) basis and the Poisson equation is solved self-consistently with integrating the gate-bias into Hamiltonian as part of pseudo-potential function[30]. Transport

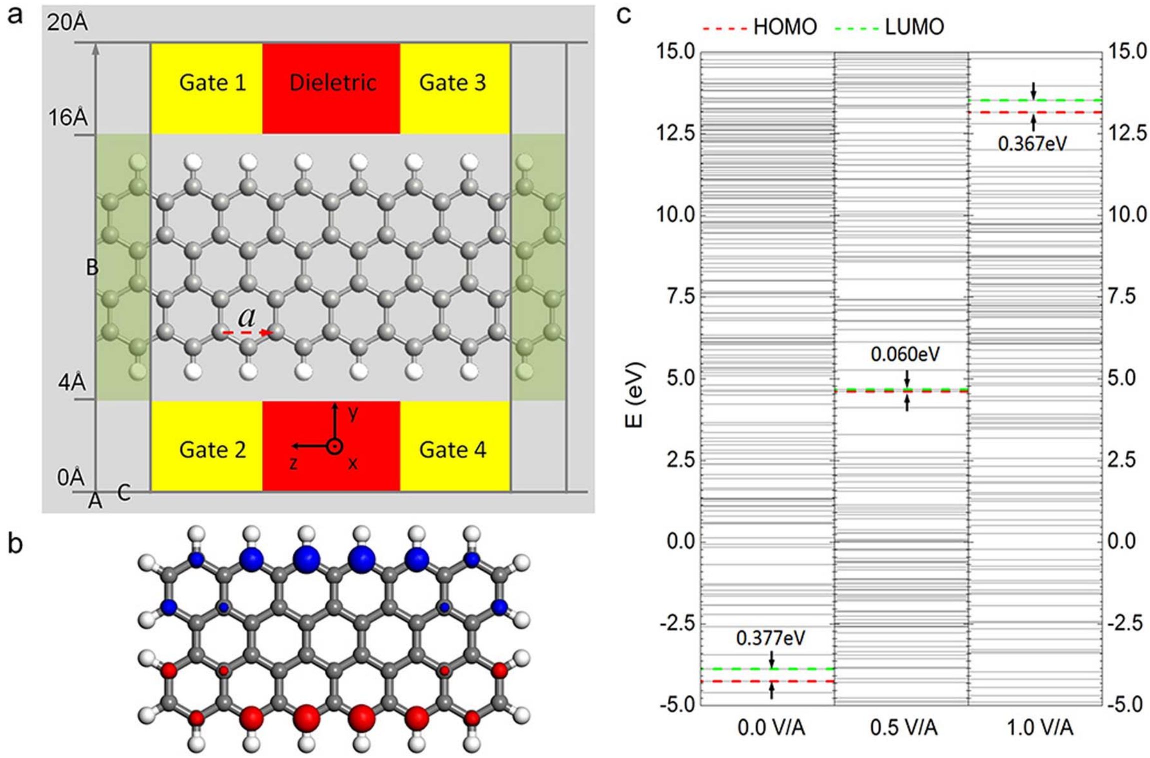

Figure 1 | Spintronic logic gate of ZGNR. Diagram of the spintronic logic gate and electronic structure of a molecule analogous to the central device of the logic gate. (a), The 4ZGNR logic gate consists of four metal $Gates_{(1,2,3,4)}$ (yellow) and two dielectric regions (red) beside the edges of the ribbon that has three parts: left electrode, device and right electrode. Because electrodes are semi-infinite long, only one primitive cell (green) is shown for each electrode in this figure. The width for metal gates and dielectric regions is 4 Å. Distance between $Gate_1$ and $Gate_2$ is 12 Å. *a* is the lattice constant of ZGNR, and 2.46 Å is used in this letter. (b), The spin density is plotted for the molecule of central device saturated by hydrogen atoms. The isovalue of the spin density is set to 0.0358 $\mu_B/Å^3$ (μ_B is Bohr magneton). α and β spins are shown in blue and red, respectively. (c), In electric field of 0.0 V/Å, 0.5 V/Å and 1.0 V/Å, energy levels of the molecule is plotted. Highest Occupied Molecular Orbital (HOMO) and Lowest Unoccupied Molecular Orbital (LUMO) are denoted by red and green dash lines. The energy gap between HOMO and LUMO is marked by black arrows. The energy gap of 0.5 V/Å is the smallest (60 meV) while the energy gaps of 0.0 V/Å and 1.0 V/Å are around 0.37 eV.

calculations are carried out in ATK package with k-point sampling of $1 \times 1 \times 100$ and the cutoff energy is set to 75 Hartree. For molecule device of 4ZGNR saturated by hydrogen atoms (Fig. 1b), the ground state is calculated by $DMol^3$ package including all electrons based on DNP (Double Numerical plus polarization) basis and LSDA functional. Based on the first principle calculations of $DMol^3$, the energy difference between the ferromagnetic ground state (-1976.518668 Hartree) and the anti-ferromagnetic ground state (-1976.519288 Hartree) is 0.62×10^{-3} Hartree (16.9 meV), and the anti-ferromagnetic state is confirmed as the ground state. As shown in Fig. 1b the molecule device is ferromagnetic ordered at each edge and anti-ferromagnetic coupled for the ground state. When there is a homogeneous in-plane external electric field (Fig. 1c), the energy gap between highest occupied molecular orbital (HOMO) and lowest unoccupied molecular orbital (LUMO) is altered and the critical field is 0.5 V/Å for which the HUMO/LUMO gap is around 60 meV and the device is near-conducting. Our result of 4ZGNR molecular device is in consistent with previous studies[4–6]. When four metal gates are built up, magnitudes of external electric field at both edges of 4ZGNR can be controlled and density distribution of opposite spins can be modulated (Fig. 2). Non-equivalent localization resulted from applied in-plane bias raises distinct blockade for opposite spins and leads to asymmetric transmission spectra. In our prototype, input and output signal of the logic gate are defined as bias on metal gate and spin-polarized transmission of electrons from left electrode to right electrode, respectively. The distance between $Gate_1$ and $Gate_2$ is 12 Å. If a 12 V bias is applied on one metal gate, then the electric field nearby this gate is around 0.5 V/Å which tunes the device into the near-conducting state, whereas the field becomes a little larger than 0 V/Å when zero bias is applied because the metal gates interact with the 4ZGNR and an effective electric field is induced due to redistribution of electrons. For input, 12 V and 0 V are used to represent 1 and 0 of Boolean algebra. It is expected that specific voltages will be used for different devices.

Gate configurations of input bias are denoted as $\{V_1,V_2,V_3,V_4\}$ (V_i is the voltage of $Gate_i$ in unit of Volt, i=1,2,3,4). There is a transmission selection rule and this rule is related to the wavefunction symmetry. There are 16 (2^4) gate configurations in total. Only seven of them are irreducible due to both the mirror symmetries of atomic structure along axis and the time-reversal symmetry of spin. For symmetric configurations, outputs are the same. Seven irreducible configurations are: {0,0,0,0}, {0,0,0,12}, {0,0,12,12}, {0,12,0,12}, {0,12,12,0}, {0,12,12,12}, {12,12,12,12} (Fig. 2 a–g). Conducting states locate at edges, so only channels at edge are effective for transmission around E_F. The metal gates next to the edges change the boundary conditions of the Poisson equation for electrostatic potential of Hamiltonian, and the electrostatic potential changes the effective electric field in both the electrodes and the central region. It is the inhomogenous effective electric field that changes the distribution of spin density in the transport system. For configuration of {0,0,0,0}, both forward transmission and backscattering are weak because both top and bottom edges are semiconducting, and transmissions of opposite spins are both nearly zero. The two transmission spectra of opposite spins are non-degenerate because there is a nonzero effective field between metal gates and 4ZGNR even under zero bias. For configuration of {0,0,0,12}, the top edge is semiconducting and

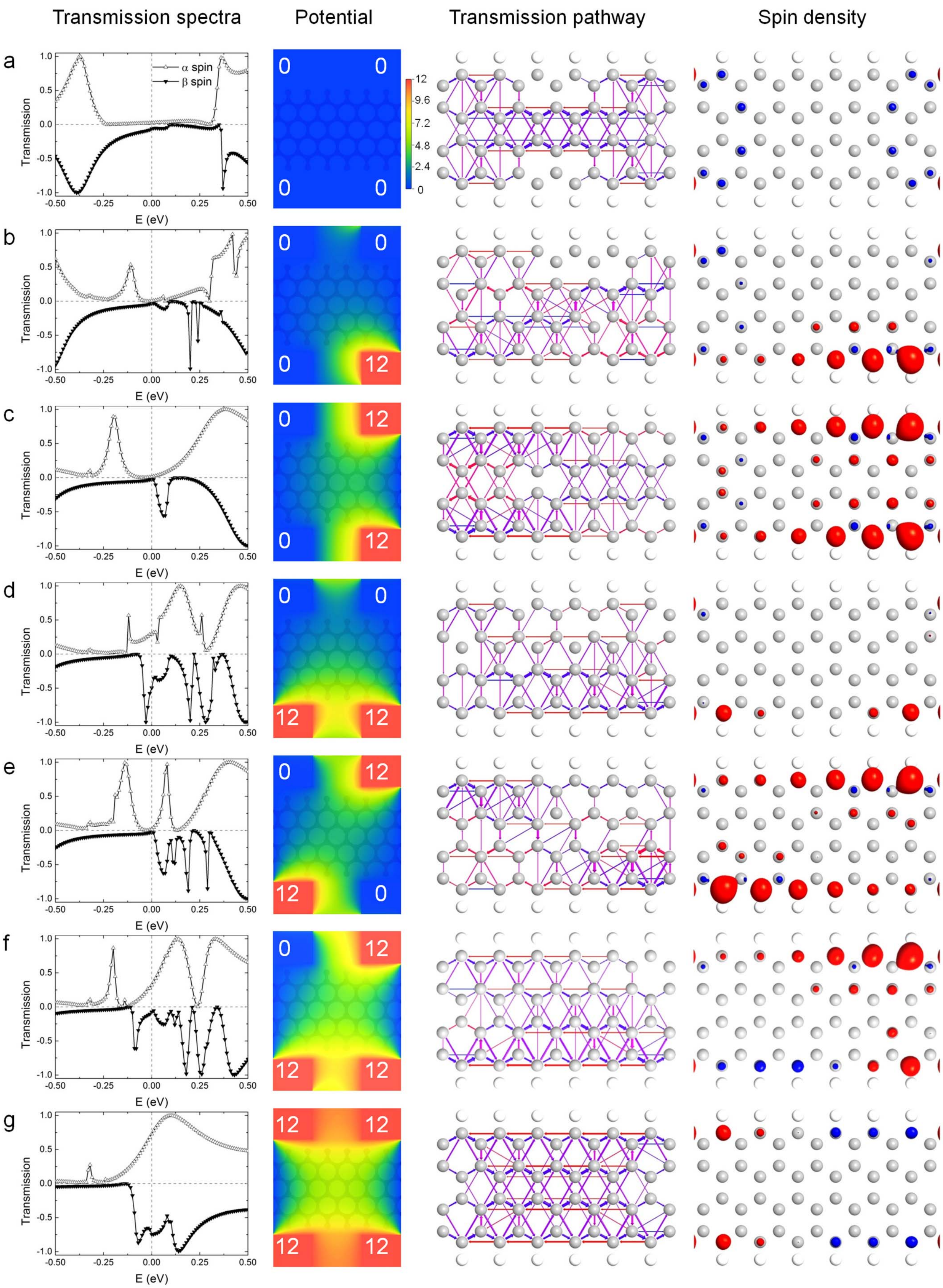

Figure 2 | Transport properties of the spintronic logic gate. Columns from left to right refer to spin-polarized transmission spectra in unit of e^2/h, external potential of metal gates, transmission pathway and spin density. In the first column, transmission of α and β spins are denoted as grey up-triangle and dark down-triangle, respectively. In the second column, the bias of metal gates are displayed and color map shows the corresponding electrostatic potential with respect to the color legend from 0 V to 12 V. In the third column, blue arrows denote forward transmission from left electrode to right electrode, whereas red arrows denote backscattering. In the fourth column, density of α and β spins are displayed in blue and red, respectively. Rows from a to e refer to the seven irreducible combinations of bias on metal gates.

Table 1 | Input and output of the spintronic logic gate. Bias on metal $Gate_{1(2,3,4)}$ shown in Fig. 1a is denoted as $V_{1(2,3,4)}$ in unit of Volt. $T_{\alpha(\beta)}$ is the transmission of α(β) spin electrons propagating from left electrode to right electrode. $T_{\alpha+\beta}$ is the total transmission. *L* is the logic value of *T* relative to a reference T_{ref}. 1 and 0 of Boolean algebra are corresponding to $T > T_{ref}$ and $T < T_{ref}$, respectively

Gate Bias (Volt)										
V_1	V_2	V_3	V_4	T_α	L_α (T_{ref}=0.1)	T_β	L_β (T_{ref}=0.1)	$T_{\alpha+\beta}$	$L_{\alpha+\beta}$ (T_{ref}=0.1)	$L_{\alpha+\beta}$ (T_{ref}=0.6)
0	0	0	0	0.026	0	0.061	0	0.087	0	0
0	0	0	12	0.005	0	0.032	0	0.038	0	0
0	0	12	12	0.017	0	0.025	0	0.042	0	0
0	12	0	12	0.297	1	0.511	1	0.808	1	1
0	12	12	0	0.023	0	0.029	0	0.051	0	0
0	12	12	12	0.323	1	0.074	0	0.397	1	0
12	12	12	12	0.728	1	0.748	1	1.476	1	1

Table 2 | Boolean algebra of the spintronic logic gate: 'AND', 'OR', 'NOT'. L_β (T_{ref}=0.1) in Table 1 is used as the output signal of the device. For inputs (denoted as L_{in}), 1 and 0 of Boolean algebra are corresponding to 12 V and 0 V on metal gates. For outputs (denoted as L_{out}), 1 and 0 of Boolean algebra are corresponding to transmission of β spin greater than and less than 0.1. Combinations of bias on metal gates form all base logic functions in the same device

.AND.			.OR.			.NOT.	
{$V_{in1}=V_1=V_2, V_{in2}=V_3=V_4$}			{$V_{in1}=V_1=V_3, V_{in2}=V_2=V_4$}			{$V_1=V_3=12, V_2=0, V_{in}=V_4$}	
L_{in1}	L_{in2}	L_{out}	L_{in1}	L_{in2}	L_{out}	L_{in}	L_{out}
0	0	0	0	0	0	0	1
0	1	0	0	1	1	1	0
1	0	0	1	0	1		
1	1	1	1	1	1		

transmission along the bottom edge is blockaded due to varying chemical potential from left to right which results in a localized spin density for β. For configuration of {0,0,12,12}, both forward transmission and backscattering are blockaded due to the mutative chemical potential from left to right. For configuration of {0,12,0,12}, the top edge is semiconducting whereas the bottom edge is close to metallic, so there is one effective channel at bottom edge and the transmission of α spin is around 0.3 whereas the transmission of β spin is greater than 0.5 because it is close to the resonant peak of transmission at energy of −0.03 eV. For configuration of {0,12,12,0}, both edges are backscattered. For configuration of {0,12,12,12}, the top edge is backscattered and the bottom edge is nearly metallic. However, the backscattering of β spin is much heavier than that of α spin due to its very localized spin density, so the transmission of β spin is small. For configuration of {12,12,12,12}, channels at both edges are open because the localization of spin density is weak, and as a result the transmission is big for both α and β.

For output, a transmission is set as reference T_{ref}, so larger and smaller transmission are corresponding to 1 and 0 of Boolean algebra, respectively. Both spin-polarized and total transmission can function in specific logic operations which depend on the reference transmission. For example, the logic operation of $T_{\alpha+\beta}$ is different between T_{ref}=0.1 and T_{ref}=0.6 (Table 1). There is also a remarkable difference in output for opposite spins. In {0,12,12,12}, logic value of output is 1 for α spin whereas it is 0 for β spin. Thus, all base logic functions are built up in the same device (Table 2) and opposite spins can perform separate logic operations simultaneously. Except for {0,0,0,12} and {0,12,12,0}, the other five irreducible configurations are used for logic operations in the prototype and T_β is preferable for output of the logic gate because it has the highest on/off ratio (~7) in 'NOT' operation.

In summary, we present a prototype of spintronic logic gates consisting of 4ZGNR and four metal gates in this letter, and the prototype can function in all base logic operations when specific combinations of bias are applied on metal gates. The mechanism lies in that, at each edge of 4ZGNR, the ferromagnetic ordered edge state around E_F can be controlled and modulated by a localized external electric field. Combinations of bias make the 4ZGNR running spintronic calculations as a logic gate. For wider ZGNR, the critical external electric field is smaller, thus quantum logic gates of wider ZGNR will use voltages lower than 12 V as their inputs and decrease the energy consuming. For our spintronic logic gate, the inputs are represented by voltages and the outputs are represented by transmission coefficients. The transmission coefficients are corresponding to the possibility of successful electron transmission through the device from the left electrode to the right electrode and thus the coefficients represent the transmission current of quantum transport. To make a real integrated circuit, there are two methods to convert the output signals to input signals. The first method is to use a classical current-voltage converting device such as a current transducer to transduce the current signal to voltage signal as inputs of other devices. The second method is to build up a spintronic current-voltage transducer which would distinguish signals of spin-current directly. Based on the prototype in this letter, it is possible to design an integrated quantum device making more advanced calculations than Boolean algebra, like quantum CPUs.

1. Feynman, R. P. Simulating physics with computers. *Int. J. Theor. Phys.* **21**, 467–488 (1982).
2. Igor, Z., Jaroslav, F. & Das Sarma, S. Spintronics: Fundamentals and applications. *Rev. Mod. Phys.* **76**, 323–410 (2004).
3. Supriyo, D. & Biswajit, D. Electronic analog of the electro-optic modulator. *Appl. Phys. Lett.* **56**, 665 (1990).
4. Behtash, B. A., Deepanjan, D., Sayeef, S. & Supriyo, D. Proposal for an all-spin logic device with built-in memory. *Nature Nanotechnol.* **5**, 266–270 (2010).
5. Castro Neto, A. H., Guinea, F., Peres, N. M. R., Novoselov, K. S. & Geim, A. K. The electronic properties of graphene. *Rev. Mod. Phys.* **81**, 109–162 (2009).
6. Young-Woo, S., Marvin, L. C. & Steven, G. L. Half-metallic graphene nanoribbons. *Nature* **444**, 347–349 (2006).
7. Elias, R., Pawe, S. & Yi, L. Nonlocal Exchange Interaction Removes Half-Metallicity in Graphene Nanoribbons. *Nano Lett.* **7**, 2211–2213 (2007).

8. Er-Jun, K., Zhenyu, Li, Jinlong, Y. & Jianguo, H. Will zigzag graphene nanoribbon turn to half metal under electric field? *Appl. Phys. Lett.* **91**, 243116 (2007).
9. Igor, Z. & Michael, F. A path to spin logic. *Nature Phys.* **1**, 85–86 (2005).
10. David, D. A. & Michael, E. F. Challenges for semiconductor spintronics. *Nature Phys.* **3**, 153–159 (2007).
11. Alexander, A. K., Jens, W., Bruno, C. & Roland, W. Realizing All-Spin–Based Logic Operations Atom by Atom. *Science* **332**, 1062 (2011).
12. Nihar, M. *et al*. Nanotomy Based Production of Transferrable and Dispersible Graphene-Nanostructures of Controlled Shape and Size. *Nature Commun.* **3**, 844–851 (2012).
13. Dmitry, V. K. *et al.* Longitudinal unzipping of carbon nanotubes to form graphene nanoribbons. *Nature* **458**, 872–876 (2009).
14. Liying, J., Li, Z., Xinran, W., Georgi, D. & Hongjie, D. Narrow graphene nanoribbons from carbon nanotubes. *Nature* **458**, 877–880 (2009).
15. Tongay, S. *et al.* Drawing graphene nanoribbons on SiC by ion implantation. *Appl. Phys. Lett.* **100**, 073501 (2012).
16. Nikolaos, T., Csaba, J., Mihaita, P., Harry, T. J. & Bart, J. van Wees. Electronic spin transport and spin precession in single graphene layers at room temperature. *Nature* **448**, 571–574 (2007).
17. Melinda, Y. H., Barbaros, O., Yuanbo, Z. & Philip, K. Energy Band-Gap Engineering of Graphene Nanoribbons. *Phys. Rev. Lett.* **98**, 206805 (2007).
18. Ponomarenko, L. A. *et al*. Chaotic Dirac Billiard in Graphene Quantum Dots. *Science* **320**, 356–358 (2008).
19. Oleg, V. Y., Katsnelson, M. I. Magnetic Correlations at Graphene Edges: Basis for Novel Spintronics Devices. *Phys. Rev. Lett.* **100**, 047209 (2008).
20. Sepioni, M. *et al*. Limits on Intrinsic Magnetism in Graphene. *Phys. Rev. Lett.* **105**, 207205 (2010).
21. Kathleen, M. M., Adrian, G. S., Wei, H., Jaroslav, F. & Roland, K. K. Magnetic Moment Formation in Graphene Detected by Scattering of Pure Spin Currents. *Phys. Rev. Lett.* **109**, 186604 (2012).
22. Nair, R. R. *et al.* Dual origin of defect magnetism in graphene and its reversible switching by molecular doping. *Nature Commun.* **4**, 2010–2015 (2013).
23. Young, A. F. *et al.* Tunable symmetry breaking and helical edge transport in a graphene quantum spin Hall state. *Nature* **505**, 528–532 (2014).
24. Sevincli, H., Topsakal, M., Durgun, E. & Ciraci, S. Electronic and magnetic properties of 3d transition-metal atom adsorbed graphene and graphene nanoribbons. *Phys. Rev. B* **77**, 195434 (2008).
25. Longo, R. C., Carrete, J., Ferrer, J. & Gallego, L. J. Structural, magnetic, and electronic properties of Ni_n and Fe_n nanostructures (n=1–4) adsorbed on zigzag graphene nanoribbons. *Phys. Rev. B* **81**, 115418 (2010).
26. Yan, L., Wei, Z., Markus, M. & Riccardo, M. Electronic and Magnetic Properties of Zigzag Graphene Nanoribbons on the (111) Surface of Cu, Ag, and Au. *Phys. Rev. Lett.* **110**, 216804 (2013).
27. Lehtinen, P. O., Foster, S., Yuchen, M., Krasheninnikov, V. & Nieminen, R. M. Irradiation-Induced Magnetism in Graphite: A Density Functional Study. *Phys. Rev. Lett.* **93**, 187202 (2004).
28. Bing, H., Feng, L., Jian, W., Bing-Lin, G. & Wenhui, D. Suppression of spin polarization in graphene nanoribbons by edge defects and impurities. *Phys. Rev. B* **77**, 153411 (2008).
29. Vosko, S. H., Wilk, L. & Nusair, M. Accurate spin-dependent electron liquid correlation energies for local spin density calculations: a critical analysis. *Can. J. Phys.* **58**, 1200 (1980).
30. Jeremy, T., Hong, G. & Jian, W. Ab initio modeling of quantum transport properties of molecular electronic devices. *Phys. Rev. B* **63**, 245407 (2001).

Acknowledgments

This research is supported by the National Natural Science Foundation of China (Grant No. 11147142, 11204201).

Author contributions

W.X.Zhang wrote the main manuscript text and prepared display items (figures and tables). All authors reviewed the manuscript.

Additional information

Competing financial interests: The authors declare no competing financial interests.

How to cite this article: Zhang, W.X. Voltage-driven spintronic logic gates in graphene nanoribbons. *Sci. Rep.* **4**, 6320; DOI:10.1038/srep06320 (2014).